Microstructural model for a three-dimensional fiber network

DEWEI QI

ABSTRACT

A three-dimensional (3-D) anisotropic angular-distribution function (ADF) was developed to quantitatively characterize fiber orientation in paper. The ADF uses five independent coefficients to characterize 3-D fiber orientation in machine-made papers. By applying the ADF to a 3-D microstructural model of paper, it is possible to predict the nine elastic constants that describe paper in three dimensions. Modelings for both machine-made paper and handsheets are presented. Young's modulus and Poisson ratio were obtained in the machine, cross-machine, and thickness directions for six machine-made papers and six handsheets over a range of z-directional orientation. The ratio E_{11}/E_{33} decreased with increasing fiber orientation in the z-direction, with the ratio dropping dramatically at small angles of z-directional orientation. Also, one of the ADF coefficients serves as a global ordering parameter to determine the degree of z-directional orientation.

Application:

A mathematical model to facilitate design of mechanical properties in the thickness direction of paperboard.

CONTROLLING SHEET STRUCTURE in the thickness direction (z-direction) is key to production of high-performance papers for coating, converting, and printing (1–3).

Papers commonly experience tensile strain perpendicular to the plane of the paper. For example, the process of separating a printing plate or blanket from the paper exerts a pull on the sheet surface. The force of the pull depends on the tackiness of the ink, the rate at which the plate is removed, the angle of separation, and other factors. If the surface fibers or coating on the sheet are not bonded strongly enough to the sheet, they will be pulled out, or picked, during the plate-separation process. Also, surface roughness and the compressibility in the *z*-direction of paper play a major role in determining print quality. The surface strength, roughness, and compressibility are greatly affected by pore structure, fiber bonding strength, and bonding structures in the thickness direction.

With rapid development of various industries and an increase of trade with Asian and East European countries, more and more papers and paperboards are being used as packaging and wrapping materials. High tensile strength and shear strength in the thickness direction are critical for packaging materials. These issues are becoming increasingly important for a U.S. paper industry in competition with world markets.

Our goal is to understand the fundamental effects of *z*-directional microstructure of paper on sheet mechanical properties in the *z*-direction. Although a vast amount of knowledge has been accumulated for paper properties measured in the sheet plane direction, little is known about those properties in the thickness direction. Traditionally, paper is treated as a two-dimensional (2-D) model in which fibers randomly lie in a plane *(4–7)*. For a machine-made paper, a 2-D distribution function is introduced to take into account the microstructural difference between the machine direction (MD) and the cross-machine direction (CD). Many theoretical and experimental studies on the 2-D angular-distribution function have been conducted since 1952, when Cox *(8)* used a Fourier function to describe the distribution of fibers. Since then, the elliptical *(9)*, cosine *(10)*, bimodal cardioid, wrapped Cauchy *(11)*, and Von Mises *(12)* functions have been proposed as the distribution function. Schulgasser *(11)* compared these various functions and found that the wrapped Cauchy distribution is best able to predict the observed mechanical properties of paper.

However, in the real world, paper is a three-dimensional (3-D) structure. Some mechanical properties—such as thickness-directional (*z*-directional) tensile strength and shear strength—largely depend on the *z*-directional distribution of fibers, particularly for high-grammage machine-made papers, if not for lab-made papers. Habeger, Mann, and Baum *(13–15)* found that paper could adequately be described as an orthotropic material. If nine elastic properties are known, the three-dimensional elastic response of the paper to applied stresses can be computed. Such information is necessary to characterize the end-use behavior of paper and for use in modeling containers or other structures. Acoustic methods have been successfully developed for measuring the nine elastic properties necessary to describe paper in three dimensions *(14, 16, 17)*.

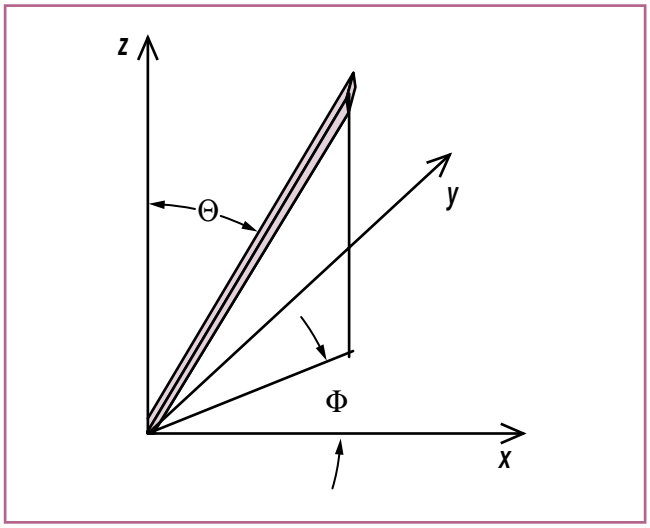

1. Coordinate system for the fiber network

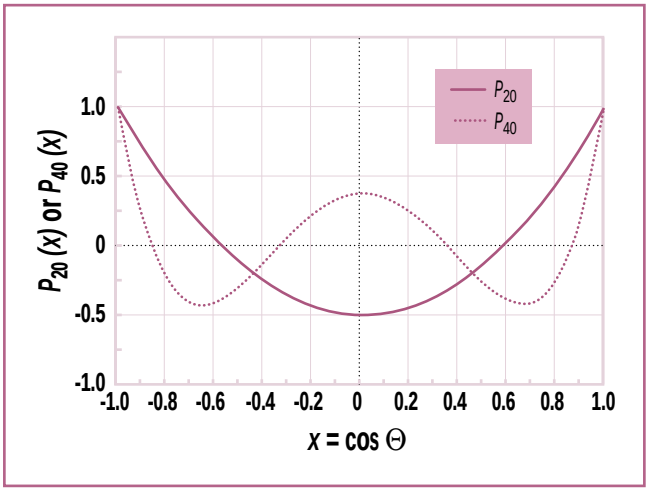

2. $P_{20}(x)$ and $P_{40}(x)$ as a function of $x = \cos\theta$

Nevertheless, progress on micromechanical modeling of paper in 3-D space has been very slow. Cox's 2-D model and 3-D isotropic model have been used for more than 40 years. A microstructural model corresponding to a 3-D anisotropic machine-made paper still is not available, although the nine elastic constants have been measured in the laboratory. To fill this gap, a 3-D angular-distribution function (ADF) has been developed to characterize the fiber orientations quantitatively for machine-made paper *(18)*. Consequently, the nine elastic moduli have been predicted analytically by using the 3-D ADF and microstructural model.

In the next section of this paper, the derivation of the 3-D ADF is given. After that, the discussion moves on to develop a *z*-directional ordering parameter that can be used to measure the degree of *z*-directional orientations of the fibers. Finally, as an application of the ADF, infinite-fiber-length and finite-fiber-length models of paper are presented in 3-D space. The analytic derivation for the elastic constants in the machine-made paper is given in terms of single fiber properties and the ADF. Modelings for both the machine-made paper and the handsheets are then conducted.

3-D ANGULAR-DISTRIBUTION FUNCTION

In general, the density of fibers in paper (number of fibers per unit volume), $\rho(r,\theta,\phi)$, is a function of position r in the paper and polar angle (θ,ϕ), as shown in **Fig. 1.** If the density of fibers depends only on the orientation of fibers, not on the position of the fibers, then the density can be written as

$$\rho(\mathbf{r},\theta,\phi) = \rho_0 f(\theta,\phi)$$

where

ρ_0 = average number of fibers per unit volume

$f(\theta,\phi)$ = angular-distribution function, defined as the possibility of finding a fiber per unit solid angle at polar angle (θ,ϕ).

Thus

$$f(\theta,\phi) = (1/n)\sum_i \delta(\cos\theta - \cos\theta_i)\,\delta(\phi - \phi_i) \quad (1)$$

may be directly measured from laboratory equipment. In Eq. 1,

δ = Dirac delta function *(19)*

n = number of fibers

i = indicates the ith fiber in the system.

The ADF can be expanded in the series of spherical harmonic functions

$$f(\theta,\phi) = \sum_{l=0}^{l=\infty}\sum_{m=-l}^{m=l} Q^*_{lm}\, Y_{lm}(\theta,\phi) \quad (2)$$

where

l and m = integers

Q^*_{lm} = coefficients in complex numbers

$Y_{lm}(\theta,\phi)$ = spherical harmonic functions.

It is more convenient to write the ADF in a real space *(19)*, i.e.,

$$f(\theta,\phi) = \sum_{l=0}^{l=\infty}\sum_{m=-ll}^{m=l} [Q^c_{lm}\, Y^c_{lm}(\theta,\phi) + Q^s_{lm}\, Y^s_{lm}(\theta,\phi)] \quad (3)$$

where Q^c_{lm} and Q^s_{lm} are expansion coefficients. The variables Y^c_{lm} and Y^s_{lm} are defined in Eqs. 4 and 5, respectively.

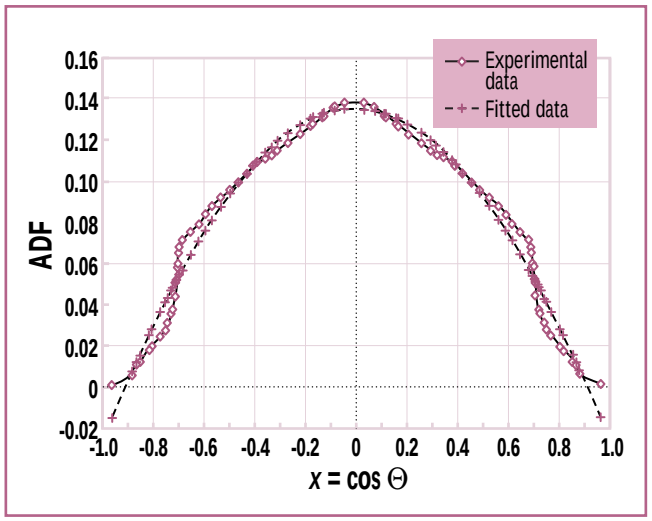

3. Projection of ADF on the y–z plane (CD), derived from experimental data, as a function of x = cos θ and the fitted curve

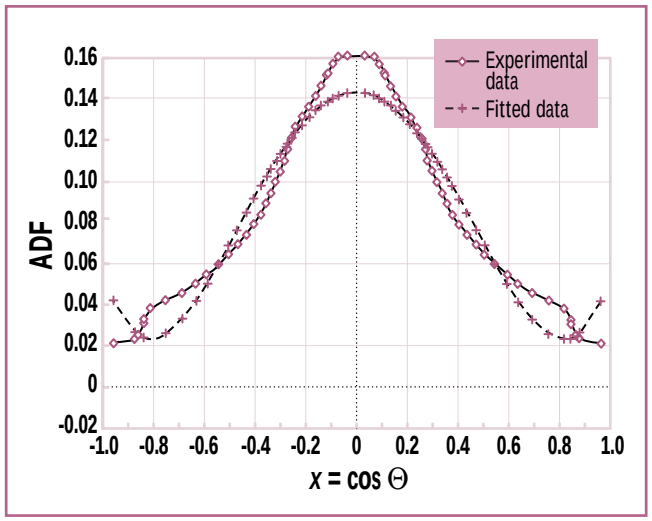

4. Projection of ADF on x–z plane (MD), derived from experimental data, as a function of x = cos θ and the fitted curve

$$Y^{c}_{lm} = P_{lm}(\cos\theta)C_m(\phi) \qquad (4)$$

$$Y^{s}_{lm} = P_{lm}(\cos\theta)S_m(\phi) \qquad (5)$$

where $P_{lm}(\cos\theta)$ is a normalized Associated Legendre function. The variable C_m is defined in Eqs. 6 and 7, and the variable S_m is defined in Eq. 8.

$$C_m(\phi) = [1/(\pi)^{1/2}]\cos m\phi,\ m \neq 0 \qquad (6)$$

$$C_0 = 1/(2\pi)^{1/2} \qquad (7)$$

$$S_m(\phi) = [1/(\pi)^{1/2}]\sin m\phi \qquad (8)$$

Substituting Eq. 1 into Eq. 3, multiplying the result by Y^{c}_{lm} or Y^{s}_{lm}, integrating both sides of this equation, and making use of the orthogonality properties of the basis functions, one obtains Eqs. 9 and 10:

$$Q^{c}_{lm} = (1/n)\sum_{i} P_{lm}(\cos\theta_i)C_m(\phi_i) \qquad (9)$$

$$Q^{s}_{lm} = (1/n)\sum_{i} P_{lm}(\cos\theta_i)S_m(\phi_i) \qquad (10)$$

Because of the orthogonality of harmonic functions, the terms with $l > 4$ do not contribute any physical property to the paper (see Appendix A). Therefore, the series is truncated at $l = 4$. Furthermore, if a symmetrical invariance of inversion for the fiber network is imposed, all odd l terms can be deleted because the parity of the spherical harmonic functions is l. Assuming that the fiber-orientational distribution is symmetric with respect to the midplane, MD, and CD of the sheet, all terms that contain $\sin m\phi$ can be dropped. (Thus the superscripts s and c in coefficients Q^{s}_{lm} and Q^{c}_{lm} are dropped from now on.) Therefore, the 3-D ADF for machine-made paper is

$$f(\theta,\phi) = (1/4\pi) + [Q_{20}P_{20}(\cos\theta)C_0] + [Q_{40}P_{40}(\cos\theta)C_0] + [Q_{22}P_{22}(\cos\theta)C_2(\phi)] + [Q_{42}P_{42}(\cos\theta)C_2(\phi)] + [Q_{44}P_{44}(\cos\theta)C_4(\phi)] \qquad (11)$$

Five independent coefficients—Q_{20}, Q_{40}, Q_{22}, Q_{42}, and Q_{44}—are required to describe the orientation of fibers in the machine-made paper in the 3-D space. Assuming angular distribution of fibers is isotropic in the x–y plane, such as in handsheets, allows one to focus on only the z-directional distribution of fibers. In this case, the ADF is reduced to a simpler form requiring only two coefficients, as seen in Eq. 12.

$$f(\theta,\phi) = (1/4\pi) + [Q_{20}P_{20}(\cos\theta)C_0] + [Q_{40}P_{40}(\cos\theta)C_0] \qquad (12)$$

Only two independent coefficients, Q_{20} and Q_{40}, are needed for this case. In particular, Q_{20} can be used to measure the degree of the z-directional orientation of the fiber network. I call it the z-directional ordering parameter of the fibers and will address it later. I have assumed that the z-axis of the coordinate system traditionally coincides with the thickness direction of the paper.

Note that the method of normalizing $f(\theta,\phi)$ here is different from that used by Cox *(8)*. The first term of the ADF in the present work is $1/4\pi$ rather than $1/2\pi$ *(8)*. However, the final results for the mechanical properties do not depend on the method of normalizing $f(\theta,\phi)$ and should be the same.

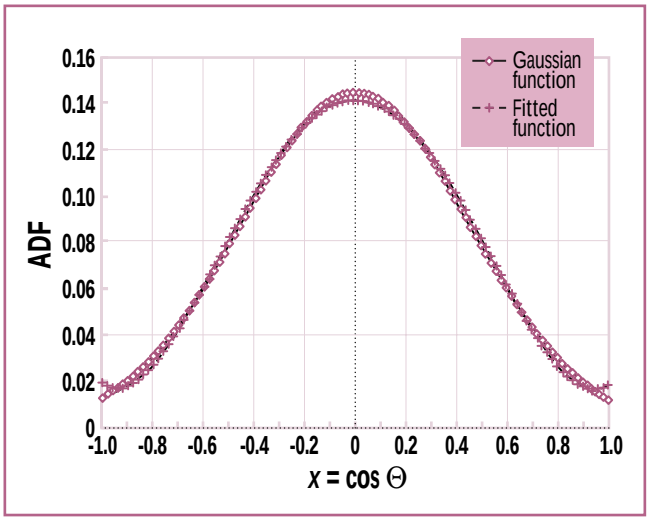

5. Fitted curve and Gaussian function with $\sigma_0 = 0.45$

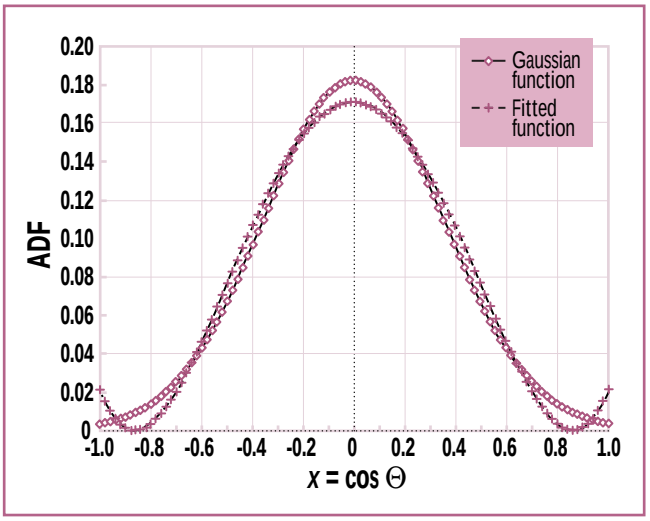

6. Fitted curve and Gaussian function with $\sigma_0 = 0.35$

Z-DIRECTIONAL ORDERING PARAMETER

If fibers are uniformly and randomly distributed in a 3-D space, then the symmetry of this paper is completely spherical. In turn, all expansion coefficients, Q_{lm} in Eq. 11, are equal to zero except the first term, which is equal to $1/4\pi$, and the physical properties of the paper are isotropic. However, in reality, the fibers are ordered in some way, by fluid flows in the headbox, by the drainage process, by the motion of wire, or by the felt moving in the MD during the papermaking process. As a result, paper is a sort of random fiber network with a certain degree of fiber aligning order that depends on the processes of papermaking. With this in mind, expansion coefficients Q_{lm} are no longer equal to zero. The ordering of fibers in the random system contributes anisotropic properties to the paper in the MD, CD, and thickness (z-direction) through these nonzero expansion coefficients.

It is very useful to define a global parameter to characterize the degree of z-directional ordering of fibers quantitatively. The coefficient Q_{l0} is calculated from Eq. 9 by averaging $P_{l0}(\cos\theta)$ over all the local fibers in the system. Consequently, statistical meaning is instinctively attached to the global coefficient Q_{l0}. It is remarkable that Q_{20} and Q_{40} ($m = 0$ in Eq. 9) among all Q_{lm} are associated with the fiber polar angle θ only and are independent of the in-plane angle ϕ. Can one take them as ordering parameters to measure the degree of the z-directional orientation of the fibers? To answer this question, both $P_{20}(\cos\theta)$ and $P_{40}(\cos\theta)$ are plotted as a function of the variable $x = \cos\theta$ in **Fig. 2.** It is clear that the value of $P_{20}(x)$ increases monotonically with the absolute value of x, while that of $P_{40}(x)$ does not. For example, if all fibers lie in the x–y plane, i.e., $x = \cos\pi/2 = 0$ in the coordinate system shown in Fig. 1, then $P_{20}(x) = -0.5$. This corresponds to the lowest z-directional ordering. Indeed, the z-directional ordering is zero for the case. If all fibers are parallel with the z-axis, i.e., $x = (0) = \pm 1$, then $P_{20}(x) = 1$. This means that the fibers have the largest z-directional ordering. It is concluded that only Q_{20}, which is directly linked to the local parameter $P_{20}(x_i)$ by

$$Q_{20} = (C_0/n)\sum_i P_{20}(x_i)$$

from Eq. 9, can be used as an ordering parameter to measure the degree of z-directional orientation globally. In other words, the value of Q_{20} increases with increasing z-directional ordering of fibers.

The following is a good example. Hasuike *et al. (2)* reported their experimental data on a 3-D microstructure of paper obtained by serial sectioning with a microtome. However, it is impossible to derive all information for the angular distribution of a real paper based on their statistics for only 138 fiber segments. Only two projection curves of the z-directional distribution function—one on the y–z plane and the other on the x–z plane—are available from their work. The two curves do not correspond to the z-directional angular distribution of the real papers, because the projections exaggerate the z-directional distribution. Nevertheless, some useful information can be extracted from their experimental work.

Both curves were used to construct two different fiber networks of papers. Fiber network one (Case 1) is constructed by using projection curve A of Fig. 8 in the work of Hasuike *et al. (2)* as the z-directional distribution function. Fiber network

	σ_0	Q_{20}	Q_{40}
A	…	0.0	0.0
B	0.60	–0.099805	0.016633
C	0.45	–0.150064	0.042747
D	0.35	–0.206010	0.084417
E	0.30	–0.234622	0.117247
F	0.28	–0.245876	0.132680
G	0.26	–0.256775	0.149107

I. Fitted values of ADF coefficients (Q_{20} and Q_{40}) for six cases of σ_0 in handsheets

	YOUNG'S MODULUS, km				POISSON RATIO	
	E_{11}	E_{33}	G_{12}	G_{23}	ν_{12}	ν_{23}
A	875.52	875.52	350	350.21	0.25	0.25
B	1078.02	495.99	432.31	298.83	0.247	0.173
C	1185.35	326.07	476.81	260.37	0.243	0.137
D	1290.56	148.86	528.58	208.63	0.221	0.0987
E	1322.17	72.28	557.09	173.99	0.187	0.0781
F	1309.91	46.69	568.75	158.58	0.152	0.0697
G	1230.94	22.71	580.31	142.60	0.0606	0.0614

II. Calculated Young's modulus and Poisson ratio for Cases A–G (handsheets)

	E_{11}/E_{33}	G_{12}/G_{13}
A	1.0	1.0
B	2.17	1.45
C	3.64	1.83
D	8.67	2.53
E	18.30	3.20
F	28.06	3.59
G	54.20	4.07

III. Values of E_{11}/E_{33} and G_{12}/G_{13} for Cases A–G (handsheets)

two (Case 2) is made by using projection curve B from the same figure. It is assumed that the fiber network in the in-plane direction is isotropic for both cases, so that the attention is paid only to the *z*-direction orientation of the fibers. The analytic ADF can be obtained by fitting Q_{20} and Q_{40} to the projection curves according to Eq. 12. The general "linear least squares with singular value decomposition" technique *(20)* was used to optimize the fitted values of Q_{20} and Q_{40}. It has been obtained that Q_{20} and Q_{40} are –0.13957 and 0.074529, respectively, for Case 1, and –0.17035 and 0.0036436 for Case 2. The fitting results are shown for Case 1 in **Fig. 3** and for Case 2 in **Fig. 4.** The fittings are fairly good, supporting our contention that the three-dimensional ADF seems reasonable for practical use. In these two figures, both the original curves, derived from the experimental data, and the fitted curves have been normalized to 1 in 3-D space.

It is worth noting that the value of Q_{20} in Case 1 is larger than that in Case 2, indicating that the degree of *z*-directional ordering of fibers in the CD is larger than in the MD for the paper tested. Clearly, the parameter Q_{20} plays an important role in determining the degree of global *z*-directional ordering.

PREDICTION OF NINE ELASTIC CONSTANTS

Paper is a three-dimensional, randomly distributed fiber network. Macromechanical properties of the paper, such as the nine elastic constants, depend essentially on the properties of fibers and their distribution in 3-D space.

To illustrate wide usages of the 3-D ADF, it will be employed to predict mechanical properties of paper by using a microstructural model of sheets. However, the function itself is independent of the details of the model.

3-D microstructural model of paper

With Cox's model of paper *(8)*, each fiber is assumed to extend in one straight line throughout the whole body of the network and to be loaded only at its ends. In that model, fibers can transmit load only in tension. If the sheet is under the possible straining, $e_{\alpha\beta}(\alpha,\beta=x,y,z)$, then strain e_f along the fiber with polar angle (θ,ϕ) is given by

$$e_f = (\sin^2\theta \cos^2\phi\, e_{xx}) +$$

$$(\sin^2\theta \sin^2\phi\, e_{yy}) + (\cos^2\theta\, e_{zz}) +$$

$$(\sin^2\theta \cos\phi \sin\phi\, e_{xy}) +$$

$$(\sin\theta \cos\theta \cos\phi\, e_{xz}) +$$

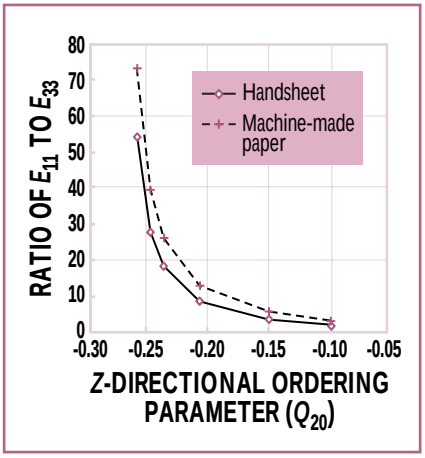

7. Ratio of E_{11} to E_{33} as a function of the z-directional ordering parameter Q_{20}. (Note: Q_{20} increases with increasing z-directional ordering.)

	σ_0	Q_{20}	Q_{40}	Q_{22}	Q_{42}	Q_{44}
H	0.60	–0.099525	0.016775	0.174994	0.0048864	0.0370663
I	0.45	–0.153860	0.042856	0.188001	–0.0274024	0.0411597
J	0.35	–0.205934	0.084461	0.200462	–0.0645980	0.0453377
K	0.30	–0.234542	0.117554	0.207304	–0.0887626	0.0477842
L	0.28	–0.245578	0.133048	0.209991	–0.099208	0.0487855
M	0.26	–0.256659	0.149623	0.212591	–0.109906	0.0497778

IV. Fitted values of ADF coefficients (Q_{20}, Q_{40}, Q_{22}, Q_{42}, and Q_{44}) for six cases of σ_0 (machine-made papers)

$$(\sin\theta\cos\theta\sin\phi\, e_{yz}) \quad (13)$$

where engineering strains are employed.

The energy density, W, can be written as

$$W = (1/2)\int_0^{\pi}\int_0^{2\pi}\sigma_f\, e_f\, V_f\, N\, f(\theta,\phi)$$

$$\sin\theta\, d\theta\, d\phi = (1/2)\int_0^{\pi}\int_0^{2\pi}$$

$$(\rho_p/\rho_f)\, E_f\, e_f^2\, f(\theta,\phi)\sin\theta\, d\theta\, d\phi \quad (14)$$

where

σ_f = stress along the fiber
V_f = volume of a single fiber
E_f = modulus of a single fiber
N = total number of fibers per unit volume
ρ_f = density of fibers
ρ_p = apparent density of paper.

Substituting Eq. 13 into Eq. 14, expanding each of the terms for sine and cosine in e_f^2 (see Eq. 13) in the series of the real spherical harmonic functions, and using their orthogonality properties, all elastic constants of the sheet can be calculated from

$$\sigma_{\alpha\beta} = \partial W/\partial e_{\alpha\beta} = C_{\alpha\beta\mu\nu}\, e_{\mu\nu} \quad (15)$$

where

α,β = x,y,z
$\sigma_{\alpha\beta}$ = stress tensor
$C_{\alpha\beta\mu\nu}$ = elastic constant tensor.

The nine elastic constants for machine-made paper have been predicted analytically in terms of fiber properties and the five coefficients. To reduce the size of this report, all formulas for the nine elastic constants are collected in Appendix B. The calculation method used here is different from and better than Cox's original procedure.

Note that if the breaking length is used as a unit of modulus, then K in Appendix B should be corrected by the apparent density of paper, i.e., $K = E_f/\rho_f$. In this way, porosity is taken into account automatically in the lowest order, and the modulus of the paper has already been corrected by the density of the paper. The other elements of the elastic matrix in Appendix B fall into zero naturally because of the symmetrical properties of the ADF. The relation between stress tensor σ and strain tensor e can be expressed as a matrix form, $\sigma = Ce$ or $e = C^{-1}\sigma$, and the various Young's moduli and Poisson ratio can be calculated.

If paper is isotropic in 3-D space, then all Q_{lm} are zero except $Q_{00}Y_{00} = 1/4\pi$, and the previous results for C_{ij} are correctly reduced to those in Cox's work *(8)*, as expected. The isotropic case is included in the present results as a special simple case. The present results are for all the anisotropic cases and are much more general than Cox's work. A commercial symbolic calculation package, MAPLE, developed by the University Waterloo *(21)*, was used to carry out both the analytic and numerical calculations.

When fibers are short and the fiber "end effects" cannot be neglected, a finite-fiber-length model should be used. Let us consider a single fiber with finite length l_0 embedded in the fiber network where fibers are bonded together. Assume that the fiber is rodlike with radius r_0 and that the mean separation of the fibers (normal to their length) is r_1. If the fiber network (sheet) is subjected to strain $e_{\alpha\beta}$, then strain e_s in the sheet along the fiber direction at a distance r_1 from the fiber centroid is governed by the same equation as in Eq. 13, except e_f is replaced by e_s. Shear stress τ may transfer from the fiber surrounding at $r = r_1$ to the fiber interface at $r = r_0$. Using a mean field method, one can calculate the elastic constant without difficulty following the similar method in the previous paragraphs. Final results for the elastic constants are similar to Eqs. 19–27 in Appendix B, where K is now replaced by

$$(E_f/\rho_f)\,\{1 - [\tanh(\lambda_0 l_0/2)/(\lambda_0 l_0/2)]$$

for the finite-fiber-length model (the unit is breaking length), where

l_0 = fiber length
λ_0 = $[H/(E_f A)]^{1/2}$
A = cross-sectional area of the fiber
H = $(2\pi G)/\ln(r_1/r_0)$
G = mean shear-transfer constant.

Modeling for handsheet

The five coefficients of the ADF can be obtained by fitting these coeffi-

	YOUNG'S MODULUS, km						POISSON RATIO		
	E_{11}	E_{22}	E_{33}	G_{12}	G_{13}	G_{23}	ν_{12}	ν_{13}	ν_{23}
H	1626.13	525.49	497.47	393.231	422.916	174.765	0.154	0.173	0.173
I	1790.82	581.92	309.45	436.657	366.191	151.39	0.151	0.135	0.135
J	1928.33	636.14	149.54	480.981	294.976	122.060	0.142	0.098 6	0.0988
K	1952.31	661.33	74.16	506.95	245.79	101.810	0.127	0.0779	0.0782
L	1919.57	665.82	48.66	517.40	223.99	92.88	0.112	0.0695	0.070
M	1758.81	653.67	24.07	528.083	201.137	83.430	0.0695	0.0616	0.0611

V. Calculated Young's modulus and Poisson ratio for Cases H–M (machine-made papers)

cients to the experimental curves of fiber distribution. Unfortunately, techniques to measure the angles of fibers in a 3-D space are not yet available. Alternatively, to focus on the *z*-directional ordering of paper, it is assumed that the angular distribution in the in-plane directions is isotropic and that the *z*-directional angles of fibers follow normal Gaussian functions with respect to $x = \cos\theta$:

$$f(\theta) = H_0\, e^{x^2/2\sigma_o^2} \qquad (16)$$

The Gaussian function is normalized to 1 by integrating x from $x = \cos\theta|_{\theta=0} = 1$ to $x = \cos\theta|_{\theta=\pi} = -1$, and H_0 is the normalized coefficient. In this way, the degree of *z*-directional orientation of fibers can be varied through parameter σ_o. Then Q_{20} and Q_{40} are fitted to the Gaussian functions by using the same technique used before *(20)*. **Figure 5** shows the fitted ADF and Gaussian function for Case C (σ_o= 0.45) and **Fig. 6** for Case D (σ_o= 0.35). The fitted values of Q_{20} and Q_{40} for six cases are collected in **Table I**. The table shows that the higher the degree of *z*-directional orientation, the larger are the values of Q_{20}. Thus the degree of fiber orientation in the *z*-direction is characterized by values of Q_{20}, and the degree of the fiber orientation in the *z*-direction decreases continuously from Case A to Case G. The validity of the ordering parameter Q_{20} is also proved from decreasing values of Q_{20} with decreasing σ_o in Table I.

The calculated results for the Young's modulus and the Poisson ratio are obtained for these cases by using the infinite-fiber-length model and presented in **Table II**. In the calculation, the apparent density, ρ_p, of paper is 720 kg/m^3, and the single fiber modulus E_f/ρ_f is 5253 km in breaking length, corrected by the assumed fiber density ρ_f = 1500 kg/m^3. The fiber modulus can also be expressed as E_f = 77.3 GPa, which corresponds to chemical pulp *(22, 23)*.

The ratio of E_{11} to E_{33} in the calculated results is 1 for isotropic Case A and 54.20 for Case G, as shown in **Table III**. The ratio rapidly increases with decreasing *z*-directional orientation of fibers, as shown in **Fig. 7**. In contrast, the ratio of G_{12} to G_{13} is 1 for Case A and 4.07 for Case G. From these results, it is clear that the ratio for tensile modulus is much more sensitive to the *z*-directional orientation of fibers than that for shear modulus.

Modeling for machine-made paper

Among the characteristics of mechanical properties of machine-made papers is that the elastic constants are different in the MD, CD, and thickness directions. The difference of fiber orientation in MD and CD has been experimentally investigated by Perkins and Mark *(24)*. In modeling the machine-made paper, it is assumed that the fiber orientation, ϕ, in MD and CD follows their results and that the *z*-directional orientation, θ, follows the same pattern as the handsheet (Eq. 16). Thus, the ADF is written as

$$f(\theta,\phi) = \{(1/2\pi) + a_2[\cos 2\phi/(\pi)^{1/2}] + a_4[\cos 4\phi/(\pi)^{1/2}]\}\, H_0\, e^{-x^2/2\sigma_o^2} \qquad (17)$$

with $x = \cos\theta$. The values for a_2 and a_4 are taken as 0.234 and 0.051, respectively, from Perkins and Mark's experimental results *(24)*. The previously described Gaussian function is normalized to 1 by integrating it from x = 1 to x = –1. Then, coefficients Q_{20}, Q_{40}, Q_{22}, Q_{42}, and Q_{44} in Eq. 11 are numerically fitted to Eq. 17. However, the fitting is carried out in the two dimensions *(20)* for variable ϕ and $x = \cos\theta$. The number of data points is 10,000 in the fitting. The fitted values of these coefficients are presented in **Table IV**. The accuracy for the two-dimensional fitting is a little bit lower than for the one-dimensional fitting. However, comparison of Tables I and IV shows that the fittings for Q_{20} and Q_{40} are within 0.3% for the handsheets and the machine-made papers..

The fitted ADF is used to calculate the nine elastic constants according to Eqs. 19–27 in Appendix B. The calculated values of Young's modulus and Poisson ratio in the *x*-, *y*- and *z*-directions are listed in **Table V**. Again, the ratio of E_{11} to E_{33}

KEYWORDS
Anisotropy, bibliographies, coefficients, distribution, elastic strength, fiber networks, fiber orientation, hand sheets, microstructure, models, paper, Poisson ratio, spheres, symmetry, three dimensional design, z direction.

	E_{11}/E_{22}	E_{11}/E_{33}	E_{22}/E_{33}	G_{12}/G_{13}	G_{12}/G_{23}
H	3.09	3.27	1.06	0.93	2.25
I	3.07	5.79	1.88	1.19	2.88
J	3.03	12.90	4.25	1.63	3.94
K	2.95	26.33	8.31	2.06	4.98
L	2.88	39.45	13.68	2.31	5.57
M	2.69	73.07	27.15	2.63	6.33

VI. Values of E_{11}/E_{33}, E_{22}/E_{11}, G_{12}/G_{13}, and G_{12}/G_{23} for Cases H–M (machine-made papers)

for the machine-made paper increases (from 3.27 for Case H to 73.07 for Case M) with decreasing *z*-directional orientation, as shown in **Table VI**. The ratio increases dramatically when most fibers are oriented at the range of small angles of *z*-directional orientation, as shown in Fig. 7. The small *z*-directional angle corresponds to θ around π/2 in the present coordinate system. Similar behavior is found for the ratio of E_{22} to E_{33}. The values of G_{12}/G_{13} and G_{12}/G_{23} also increase with decreasing *z*-directional orientation of the fibers. However, as with the handsheets, the fiber orientation affects the tensile modulus much more profoundly than it affects the shear modulus, as shown in Table VI. The ratio of Young's modulus in MD to that in CD decreases slightly with decreasing *z*-directional orientation.

Since experimental data of the angular distribution of fibers in 3-D space are not available, it is difficult to compare the theoretical results with experimental values directly. However, the main results for the Poisson ratio and for the tensile and shear moduli fall into the range of experimental results *(25)*. Only the ratio of E_{11} to E_{33} in this calculation seems still smaller for the case with very small angles of *z*-directional orientation, compared with the experimental values. This problem may be caused by inaccurate fitting. In this case, a step function should be used as an ADF, and the transversal properties of single fibers should be incorporated to remove the negative Poisson ratio (ν_{12}) obtained by Cox *(8)*. This will be included in the next report.

Nevertheless, the present work shows that the 3-D ADF can be used to predict the mechanical properties of fiber networks—ranging from isotropic Case A to anisotropic Case M—with small *z*-directional orientation.

CONCLUSIONS

An anisotropic, three-dimensional, angular distribution function (ADF) was developed to describe fiber orientation in a random fiber network. Five coefficients, Q_{20}, Q_{40}, Q_{22}, Q_{42}, and Q_{44}, are needed to describe machine-made papers. For a handsheet, where fiber angular distribution in the in-plane direction is isotropic, only two coefficients, Q_{20} and Q_{40}, are needed. Since Q_{20} increases monotonically with increasing (absolute) value of x = cos θ, Q_{20} can be used to measure the degree of the *z*-directional orientation of fibers globally. Therefore, Q_{20} is defined as a *z*-directional ordering parameter. The results presented here show that the *z*-directional ordering is larger in the CD than in the MD for a given paper.

The nine elastic moduli that describe paper in three dimensions were predicted analytically using the proposed ADF and Cox's microstructural model of paper *(8)*. Ideally, the ADF coefficients should be fitted to experimental curves. Unfortunately, such experimental data are not available. Instead, it was assumed that (a) the fiber angular distribution in the *z*-direction follows the normal Gaussian distribution—thus allowing the degree of fiber orientation in the *z*-direction to be varied through σ_0 (Eq. 16)—and (b) the angular distribution in the *x–y* plane follows experimental results in the literature. The five ADF coefficients were fitted based on these two assumptions.

The values for Young's modulus and Poisson ratio were calculated from modeling of both machine-made paper and handsheets. All values were calculated over a range of *z*-directional orientation. It was found that the ratio of E_{11} to E_{33} decreases with increasing *z*-directional orientation of fibers, dropping dramatically when the sheet has a small *z*-directional orientation. The *z*-directional orientation also affects the shear modulus, but not as sensitively as it affects the tensile modulus. Moreover, it is believed that the 3-D angular distribution can be used to describe the fiber suspensions in the headbox of the paper machine. **TJ**

Qi is an assistant professor in the Department of Paper and Printing Science and Engineering, Western Michigan University, Kalamazoo, MI 49008-3843.

The author thanks Derek H. Page for stimulating discussions.

Received for review Jan. 23, 1996.

Accepted May 9, 1996.

LITERATURE CITED

1. Baum, G. A., *Products of Papermaking* (C.F. Baker, Ed.), PIRA International, Leatherhead, UK, 1993, p.1.
2. Hasuike, M., Kawasaki, T., and Murakami, K., *J. Pulp Paper Sci.* 18(3): J114(1992).
3. Waterhouse, J. F., *Tappi J.* 67(6): 104(1984).
4. Page, D. and Seth, R. S., *Tappi* 63(6): 113(1980).
5. Schulgasser, K. and Page, D. H., *Composite Sci. Technol.* 32(4): 279(1988).
6. Perkins, R. W. and Mark, R. E., *Tappi* 59(12): 118(1976).
7. Van den Akker, J. A., "Some theoretical considerations on the mechanical properties of fibrous structures," in *Formation and Structure of Paper* (F. Bolam, Ed.), Transactions of 1961 Symposium, British Paper and Board Makers Association, London, 1962, pp. 205–41.
8. Cox, H. L., *Brit. J. Appl. Phys.* 3: 72(1952).
9. Forgacs, O. L. and Strelis, I., *Pulp Paper Mag. Can.* 64(1): T3(1963)
10. Corte, H. and Kallmes, O. J., "Statistical geometry of a fibrous network," in *Formation and Structure of Paper* (F. Bolam, Ed.), Vol. 1, Technical Section, British Paper and Board Makers Association, London, 1962, p. 13.
11. Schulgasser, K., *J. Matl. Sci.* 20: 859(1985).
12. Mardia, K. V., *Statistics and Directional Data*, Academic Press, New York, 1972.
13. Habeger, C. C., *J. Eng. Matls. Technol.* 112: 366(1990).
14. Mann, R. W., Baum, G. A., and Habeger, C. C., *Tappi* 63(2): 163(1980).
15. Baum, G. A., Brennan, D. C., and Habeger, C. C., *Tappi* 64(8): 97(1981).
16. Baum, G. A., Habeger, C. C., and Fleischman, E. H., "Measurement of the orthotropic elastic constants of paper," in *The Role of Fundamental Research in Paper Making*, Mechanical Engineering Publications, London, 1983, p. 453.
17. Brodeur, P. H., *Tappi J.* 77(3): 213(1994).
18. Qi, D. and Aidun, C. K., *TAPPI 1995 Engineering Conference Proceedings*, Book 1, TAPPI PRESS, Atlanta, p. 243.
19. Arfken, G., *Mathematical Methods for Physicists*, Academic Press, New York, 1985.
20. Press, W. H., Flannery, B. P., Teukolsky, S. A., *et al.*, *Numerical Recipes*, Cambridge U. Press, Cambridge, MA, 1989.
21. Char, B. W., Geddes, K. O., Gonnet, G. H., *et al.*, *Maple V*, Springer–Verlag, New York, 1991.
22. Subramanian, L. and Carlsson, L. A., *Tappi J.* 77(11): 209(1994); 77(12): 85(1994).
23. Page, D. H., El-Hosseiny, F., and Winkler, K., *Tappi* 60(4): 114(1977).
24. Perkins, R. W. and Mark, R. E., "Fiber geometry and mechanical properties," in *The Role of Fundamental Research in Paper Making*, Mechanical Engineering Publications, London, 1983, p. 453.
25. Baum, G. A., "Mechanical properties of paper," in *Encyclopedia of Materials Science and Engineering* (M. B. Bever, Ed.), Pergamon Press, New York, 1986, pp. 2911–16.

APPENDIX A

The highest order of the power of cos θ or sin θ or their products in e_f^2 of Eq. 14 is 4. When these terms are expanded in a series of spherical harmonic functions, the highest order of Associated Legendre functions obtained is 4 for l too. These functions are orthogonal to the ADF in Eq. 14. Therefore, any term with l higher than 4 in ADF does not contribute to the mechanical properties of the paper.

APPENDIX B

$$\begin{bmatrix} C_{11} & C_{12} & C_{13} & 0 & 0 & 0 \\ & C_{22} & C_{23} & 0 & 0 & 0 \\ & & C_{33} & 0 & 0 & 0 \\ & & & C_{44} & 0 & 0 \\ & & & & C_{55} & 0 \\ & & & & & C_{66} \end{bmatrix} \tag{18}$$

with

$$C_{11} = K\{(1/5) - [4(5\pi)^{1/2}/35]Q_{20} + [2(\pi)^{1/2}/35]Q_{40} + [4(15\pi)^{1/2}/35]Q_{22} - [4(5\pi)^{1/2}/105]Q_{42} + [2(35\pi)^{1/2}/105]Q_{44}\} \tag{19}$$

$$C_{22} = K\{(1/5) - [4(5\pi)^{1/2}/35]Q_{20} + [2(\pi)^{1/2}/35]Q_{40} - [4(15\pi)^{1/2}/35]Q_{22} + [4(5\pi)^{1/2}/105]Q_{42} + [2(35\pi)^{1/2}/105]Q_{44}\} \tag{20}$$

$$C_{33} = K\{(1/5) + [8(5\pi)^{1/2}/35]Q_{20} + [16(\pi)^{1/2}/105]Q_{40} \tag{21}$$

$$C_{44} = K\{(1/15) + [2(5\pi)^{1/2}/105]Q_{20} - [8(\pi)^{1/2}/105]Q_{40} - [2(15\pi)^{1/2}/105]Q_{22} - [4(5\pi)^{1/2}/105]Q_{42} \quad (22)$$

$$C_{55} = K\{(1/15) + [2(5\pi)^{1/2}/105]Q_{20} - [8(\pi)^{1/2}/105]Q_{40} + [2(15\pi)^{1/2}/105]Q_{22} + [4(5\pi)^{1/2}/105]Q_{42} \quad (23)$$

$$C_{66} = K\{(1/15) - [4(5\pi)^{1/2}/105]Q_{20} + [2(\pi)^{1/2}/105]Q_{40} - [2(35\pi)^{1/2}/105]Q_{44} \quad (24)$$

$$C_{12} = C_{66} \quad (25)$$

$$C_{13} = C_{55} \quad (26)$$

$$C_{23} = C_{44} \quad (27)$$

where $K = E_f(\rho_p/\rho_f)$ and subscripts of C_{ij} have been written in a traditional way rather than $C_{\alpha\beta\mu\nu}$.

WORLD WIDE WEB

How to access TAPPI online via the

1996 marks TAPPI's first anniversary online. In September 1995, the Association launched its home page on the Internet's World Wide Web to give industry members around the world access to information about TAPPI and the paper and allied industries.

Anyone with a personal computer, a modem and access to the Internet World Wide Web can access TAPPI's web site. The URL (internet address) is: http://www.tappi.org. Users can locate and access material in such broad topical areas as membership, publications, conferences, and education – all with a click of a mouse button. The TAPPI page features links to other pulp and paper industry sites as well as e-mail access to key TAPPI staff members. Information provided on the site is updated regularly.